Analysis of source regions and transport pathways of sub-micron aerosol components in Europe

Michelle Y. Schneider[1,2], Jianhui Jiang[3], Ying Chen[4], Wenche Aas[5], Samira Atabakhsh[6], Minna Aurela[7], Claudio Belis[8], Aikaterini Bougiatioti[9], Michael Bressi[8], Francesco Canonaco[10], Benjamin Chazeau[1,11], Hasna Chebaicheb[12,13,14], Mikael Ehn[15], Konstantinos Eleftheriadis[16], Olivier Favez[13,14], Harald Flentje[17], Anna Font[2,a], Evelyn Freney[18], Stefania Gilardoni[19], Maria I. Gini[16], David C. Green[2], Liine Heikkinen[15,20,21], Hannes Keernik[22], Radek Lhotka[23], Chunshui Lin[24], Marek Maasikmets[22], Nicolas Marchand[11], María Cruz Minguillón[25], Jaroslaw Necki[26], Jurgita Ovadnevaite[24], Marco Paglione[27], Julija Pauraite[28], Jean-Eudes Petit[29], Michael Pikridas[30], Stephen Platt[5], Petra Pokorná[23], Vanes Poluzzi[31], Laurent Poulain[6], Véronique Riffault[12,14], Matteo Rinaldi[27], Jean Sciare[30], Yulia Sosedova[10], Iasonas Stavroulas[9], Hilkka Timonen[7], Anna Tobler[10], Jeni Vasilescu[32], Marta Via[25,b], Petr Vodička[23], Yunjiang Zhang[33], Olga Zografou[16], Kaspar Rudolf Dällenbach[1], Abhishek Kumar Upadhyay[1], Gang I. Chen[2*], Manousos-Ioannis Manousakas[1,c*], Imad El Haddad[1], André S.H. Prévôt[1]

[1]PSI Center for Energy and Environmental Sciences, 5232, Villigen, Switzerland
[2]MRC Centre for Environment and Health, Environmental Research Group, Imperial College London, W12 0BZ, London, United Kingdom
[3]Shanghai Key Lab for Urban Ecological Processes and Eco-Restoration, 200241, Shanghai, China
[4]College of Life and Environmental Sciences, University of Birmingham, B15 2TT, Birmingham, United Kingdom
[5]NILU, Kjeller, 2007, Norway
[6]Leibniz Institute for Tropospheric Research (TROPOS), 04 318, Leipzig, Germany
[7]Atmospheric Composition Research, Finnish Meteorological Institute, 00101, Helsinki, Finland
[8]European Commission - Joint Research Centre, Unit Clean Air and Climate, 21027, Ispra, Italy
[9]Institute for Environmental Research and Sustainable Development, National Observatory of Athens, 15236, Athens, Greece
[10]Datalystica Ltd., Parkstrasse 1, 5234, Villigen, Switzerland
[11]Aix Marseille Univ, LCE, Marseille, France
[12] IMT Nord Europe, Institut Mines-Télécom, Université de Lille, Centre for Energy and Environment, 59000, Lille, France
[13]Institut National de l'Environnement Industriel et des Risques (INERIS), 60550, Verneuil-en-Halatte, France
[14]Laboratoire Central de Surveillance de la Qualité de l'Air (LCSQA), 60550, Verneuil-en-Halatte, France
[15]Institute for Atmospheric and Earth System Research/Physics , Faculty of Science, University of Helsinki, 00014, Helsinki, Finland
[16]ENRACT, Institute of Nuclear and Radiological Science & Technology, Energy & Safety, NCSR Demokritos, 15310, Athens, Greece
[17]German Meteorological Service (DWD), 82383, Observatory Hohenpeissenberg, Germany
[18]Laboratoire de Météorologie Physique, UMR6016, Université Clermont Auvergne-CNRS, 63170, Aubière, France
[19]National Research Council, Institute of Polar Sciences (CNR-ISP), 40129, Bologna, Italy
[20]Department of Environmental Science, Stockholm University, 114 18, Stockholm, Sweden
[21]Bolin Centre for Climate Research, 114 18, Stockholm, Sweden
[22]Air Quality and Climate Department, Estonian Environmental Research Centre (EERC), Marja 4D, Tallinn, Estonia
[23]Institute of Chemical Process Fundamentals, Czech Academy of Sciences, Rozvojová 1, 16500 Prague 6, Czech Republic

[24]*School of Natural Sciences, Physics, University of Galway, Centre for Climate and Air Pollution Studies, Ryan Institute, H91 CF50, Galway, Ireland*
[25]*Institute of Environmental Assessment and Water Research (IDAEA), Spanish National Research Council (CSIC), 08034, Barcelona, Spain*
[26]*AGH University of Krakow, Faculty of Physics and Applied Computer Science, 30-059, Krakow, Poland*
[27]*Italian National Research Council - Institute of Atmospheric Sciences and Climate (CNR-ISAC), 40129, Bologna, Italy*
[28]*SRI Center for Physical Sciences and Technology (FTMC), 10257, Vilnius, Lithuania*
[29]*Laboratoire des Sciences du Climat et de l'Environnement (LSCE), 91190, Gif-sur-Yvette, France*
[30]*Climate and Atmosphere Research Center (CARE-C), The Cyprus Institute, 2121, Nicosia, Cyprus*
[31]*Arpae Emilia-Romagna, Centro Tematico Regionale Qualità dell'Aria, 40139, Bologna, Italy*
[32]*National Institute of Research and Development for Optoelectronics, 077125, Magurele, Romania*
[33]*Collaborative Innovation Center of Atmospheric Environment and Equipment Technology, Jiangsu Key Laboratory of Atmospheric Environment Monitoring and Pollution Control, Joint International Research Laboratory of Climate and Environment Change, School of Environmental Science and Engineering, Nanjing University of Information Science and Technology, 210044, Nanjing, China*

[a]*Now at: IMT Nord Europe, Institut Mines-Télécom, Université de Lille, Centre for Energy and Environment 59000, Lille, France*
[b]*Now at: Now at: Center for Atmospheric Research, University of Nova Gorica, 5270 Ajdovščina, Slovenia*
[c]*Now at: ENRACT, Institute of Nuclear and Radiological Science & Technology, Energy & Safety, NCSR Demokritos, 15310, Athens, Greece*

∗Corresponding authors: Email address: gang.chen@imperial.ac.uk (Gang I. Chen), manousos.manousakas@psi.ch (Manousos-Ioannis Manousakas)

Abstract

It is important to study aerosols and their origins, as they pose various negative health and environmental impacts. In this study, we combined year-long datasets from 15 different countries with Trajectory Statistical Methods (TSMs) on such a comprehensive scale for the first time. We found possible source regions and seasonal variations of various particulate matter (PM) components, including total organic aerosol (OA), biomass burning OA (BBOA), oxygenated OA (OOA), ammonium (NH_4), nitrate (NO_3), and sulphate (SO_4) in Europe. We found that for all of the studied components, eastern Europe was among the highest contributors. For NO_3, other important source regions were northern France and the Benelux, while for SO_4, there were significant contributions from the Mediterranean region. We also compared our measurement-based model with simulated concentrations of an atmospheric chemistry transport model (CAMx). We observed a satisfactory agreement in regions where we had sufficient coverage with air pollution monitoring stations. The main deviations for OA were found around the Po Valley, where CAMx consistently estimated higher concentrations, while the TSM analysis did not highlight it as a hot spot because long-term monitoring data sets in this region are lacking. CAMx also underestimated the concentrations around Poland, mainly from residential burning. Our results provide opportunities to refine European emission inventories and deliver valuable information on long-range transported air pollutants. It suggests that policies mitigating air pollution in Eastern Europe and the Benelux could help improve overall air quality in entire Europe more efficiently.

1 Introduction

Particulate matter (PM) remains a persistent environmental challenge, with adverse effects on human health, ecological systems, and global climate (Harrison and Yin, 2000). PM varies in size and composition and is emitted from a wide range of sources, encompassing both natural and human emissions. Among the primary sources of PM are transportation, biomass burning, dust resuspension, industrial processes, and agricultural activities. The impacts of PM on human health are profound and diverse. Inhalation of PM can lead to respiratory problems such as asthma, bronchitis, and other respiratory infections (Samoli et al., 2016). Fine particulate matter, known as $PM_{2.5}$ (particles with aerodynamic diameters of 2.5 micrometres or smaller), can penetrate deep into the lungs and even enter the bloodstream, increasing the risk of cardiovascular diseases, strokes, cancers, and other systemic health issues (Mitsakou et al., 2007).

Particulate matter consists of both organic and inorganic components. Examples of the latter are sulphate, nitrate, chloride, ammonium, and black carbon. The sources and formation processes of these inorganic components are relatively understood, while the other part of PM, organic aerosols (OA), consists of thousands of compounds; therefore, their formation processes and sources remain challenging to deconvolve. Previous measurements across the world suggested that OA can dominate the overall PM mass and consist of 20–90% of the total PM mass (Chen et al., 2022; Crippa et al., 2014; Jimenez et al., 2009). Recent studies have reported an overview of OA sources in Europe by employing advanced source apportionment techniques (Calvin et al., 2023; Chen et al., 2022).

While local sources undoubtedly play a significant role in aerosol pollution, it is crucial not to overlook the substantial impact of transboundary transport. PM can travel vast distances, extending far beyond its original emission point and affecting regions remote from its sources. To better grasp the complex interactions between aerosols and long-range transport, researchers have increasingly turned to trajectory statistical methods (TSMs) (Salvador et al., 2008). These analytical techniques leverage air mass backward trajectories, which trace the path of air masses from receptor locations back to their source regions, and PM concentration data collected at various receptors (Salvador et al., 2010). While TSMs do not account for factors like atmospheric dispersion, chemical conversion, or dry and wet deposition through the Hybrid Single-Particle Lagrangian Integrated Trajectory model (HYSPLIT) (NOAA, *accessed 1.11.25*), developed by NOAA's Air Resources Laboratory. However, they offer simplicity and effectiveness in application. TSMs can assist in pinpointing relevant source regions and distinguishing the airflow patterns associated with the transport of regional and large-scale air pollution. By examining the relationship between air mass trajectories and PM concentrations, TSMs enable the identification of potential emission hotspots, the characterisation of pollutant transport pathways, and the assessment of the efficacy of regional air quality management strategies. Utilising TSMs with a large number of trajectories can notably diminish trajectory uncertainty, which arises from interpolation and truncation processes, low temporal or spatial resolution of wind data, or inadequate selection of starting heights (Lupu and Maenhaut, 2002).

Previous studies have highlighted the potential of incorporating multiple receptors in TSMs to enhance accuracy (Hsu et al., 2003; Lee and Ashbaugh, 2007). In this study, we leverage comprehensive datasets utilised in harmonised OA source apportionment across Europe to identify

potential source hotspots in the region using TSMs. This has not been done previously on this scale and with this level of high-quality source apportionment data from high-time resolution measurements (30 min to 4 hours). By integrating all datasets, trajectories converge at various receptor sites, facilitating a more robust analysis (Stohl, 1996). This convergence, together with variations in concentrations at each site, amplify the redistribution process, thereby improving efficacy. The findings from TSM-based investigations are invaluable for policymakers, environmental agencies, and public health authorities aiming to devise targeted interventions to mitigate the impacts of transboundary aerosol pollution.

2 Methodology

In this study, we used the chemical composition data and the source apportionment results of 22 air quality observational sites from 15 different countries over Europe, published in (Chen et al., 2022). In addition, 5 sites in Italy were included, some of which have been published previously in Paglione et al. (2020). An overview of the countries and the measurement periods can be found in Figure 1. Measurement devices include the Aerodyne Aerosol Mass Spectrometer (AMS) and the Aerosol Chemical Speciation Monitor (ACSM), which both deliver real-time mass concentrations of aerosol species (i.e., organic, nitrate, sulphate, ammonium, and chloride). In particular, data from 18 Q-ACSM (quadrupole ACSM (Ng et al., 2011)), 3 ToF-ACSM (time-of-flight ACSM (Fröhlich et al., 2013)), 1 C-ToF-AMS (compact time-of-flight AMS (Drewnick et al., 2005)), and 2 HR-ToF-AMS (High-Resolution ToF-AMS (Paglione et al., 2020)) were used in this study.

153 The measurements of the concentrations were averaged every 12 hours (at 12 a.m. and 12 p.m.).
154 These averaged values were used in TSMs analysis by combining them with trajectory endpoints
155 using an R script. The script can be found in the supplementary material. A statistical analysis
156 (Concentration Weighted Trajectory, CWTs) was done using the **openair** R package (Carslaw,
157 2019), an open-source tool for analysing air pollution data. The R script for the plotting can be
158 found in the supplementary material, and the results are shown in section 3.

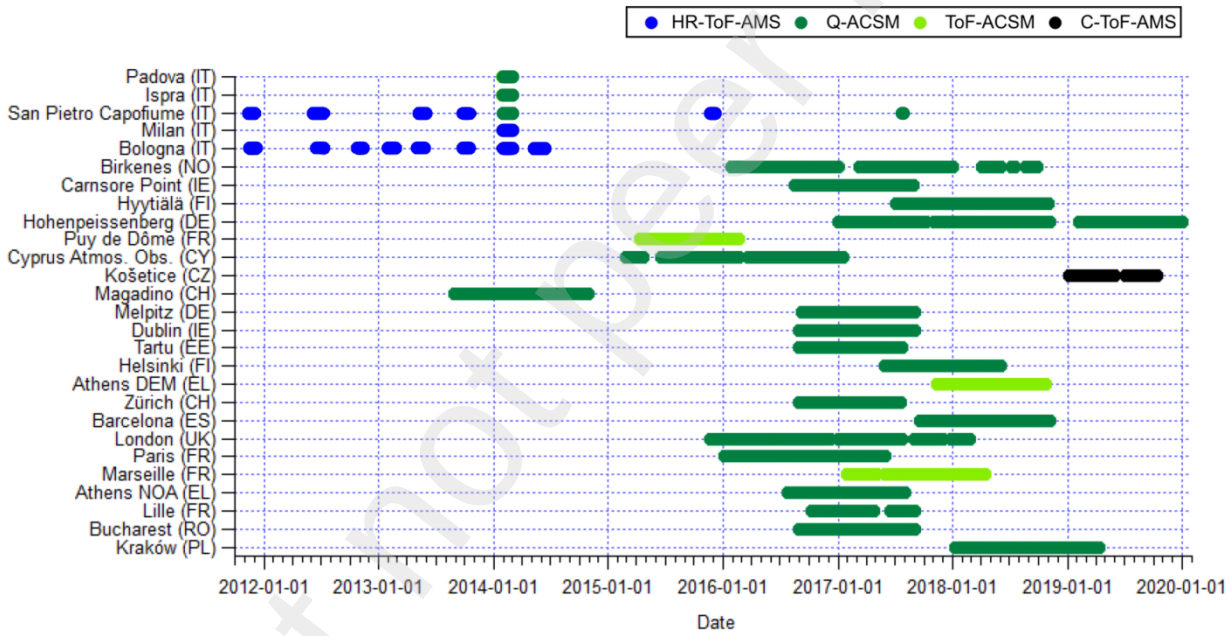

159

160 **Fig. 1.** The contributing countries and the measurement periods considered in this experiment. 24
161 ACSM measurements and 3 AMS measurements were used in this study (Chen et al., 2022;
162 Paglione et al., 2020).

163 We chose to focus on specific PM factors based on their universality, i.e., their presence in most
164 of the stations, as well as their relative importance, based on the results from Chen et al. (2022).
165 We studied two organic PM factors: biomass burning OA (BBOA) and oxygenated OA (OOA),
166 as well as total organics, i.e., the sum of all OA factors. BBOA originates mainly from residential
167 heating activities, therefore it is more regional and could be more prevalent in rural areas. OOA is

an important factor, as it makes up 70% of total OA. Rapid oxidation of primary emissions (e.g., BBOA, HOA, COA, biogenic) can be a considerable pathway of OOA formation. Consequently, biogenic OOA is more prevalent in warmer seasons, while anthropogenic OOA has larger contributions in colder seasons. In addition, OOA is expected to be transported over long distances. Other organic components resolved by Chen et al. (2022), such as traffic OA or cooking OA, were not considered, as they only exist in specific urban environments. Even more site-specific factors, such as cigarette smoke and ship industry OA, were also not considered for the same reasoning. Additionally, we also considered three inorganic PM components: ammonium (NH_4), nitrate (NO_3), and sulphate (SO_4). NH_4 contributes on average 10% of overall sub-micron aerosol. In Europe, ammonium emissions are dominated by agriculture, with some contribution from traffic exhausts (Liu et al., 2024). NO_3 has a similar overall PM contribution but shows a higher variability than NH_4, as it can make up to 30% of total aerosol. NO_3 comes from the oxidation of NO_x, which in Europe is mostly emitted from traffic and industry. SO_4 is the highest inorganic sub-micron aerosol contributor, on average 16%. Sulphate originates from the oxidation of SO_2, mainly emitted from heavy fuel oil and coal combustion (Bressi et al., 2021).

2.1 Back-trajectory analysis

The backward trajectories were modelled using HYSPLIT. It has been widely used in many previous studies to successfully investigate the impacts of atmospheric transport and dispersion all over the world (Chen et al., 2021; Escudero et al., 2011; Stein et al., 2015). For the input meteorological data, we used the GDAS (Global Data Assimilation System) global archive from 2006–present with 1-degree resolution, provided by the National Weather Service's National

189 Centres for Environmental Prediction (NCEP) (GDAS, *accessed 1.11.2025*). We used each of the
190 27 measurement stations as end points and modelled one 72-hour back-trajectory every 12 hours
191 (at 12 a.m. and 12 p.m. UTC) for the periods where the ACSM/AMS data were available, with
192 consideration of the computational capacity. The height of the trajectories arriving at the end points
193 was set to 200 metres above ground, and points in the trajectories reaching over 1500 metres above
194 ground were filtered out.

195 *2.2 Concentration weighted trajectory*

196 The **openair** package provides two kinds of statistical methods to identify possible source
197 locations by using back-trajectories: the Potential Source Contribution Function (PSCF) and the
198 Concentration Weighted Trajectory (CWT). Both methods divide the map into grid cells (i,j) and
199 can be easily applicable to multiple receptors. The PSCF method takes the number of times a
200 source concentration was high when the trajectories passed through the cell (i,j), and divides it by
201 the number of times a trajectory passed through the cell (i,j). The CWT, on the other hand,
202 calculates the mean concentration species, i.e., their logarithm, for each grid cell as follows:

203 $$\ln(\overline{C}_{ij}) = \frac{1}{\sum_{k=1}^{N} \tau_{ijk}} \sum_{k=1}^{N} \ln(c_k)\,\tau_{ijk}$$

204 where i and j are the indices of grid, k the index of trajectory, N the total number of trajectories
205 used in analysis, c_k the pollutant concentration measured upon arrival of trajectory k, and τ_{ijk} the
206 residence time of trajectory k in grid cell (i,j). With this CWT method, air packets that stay longer
207 in a cell are weighted higher, which is not the case for PSCF. Additionally, the PSCF method

requires a weighting function for multi-site analysis, which remains a challenge. Furthermore, as previously mentioned, PSCF relies on an arbitrary threshold, causing the model to emphasize high-source contributions. This can result in an imbalanced representation of moderate and relatively high source contributions. For these reasons, we have chosen to use CWT for the purpose of this study. A high value of $\overline{C}_{ij}$ means that air parcels passing over cell (i,j) would, on average, cause high concentrations at the receptor site (Carslaw, 2019; Wilks, 2019).

2.3 Simulations with CAMx

An atmospheric chemistry transport model (CAMx) (Yarwood et al., 2024) was deployed to simulate the distribution and transport of air pollutants for the year 2017. We chose that particular year because it had the largest overlap of the ACSM/AMS data (see Figure 1), making it more suitable for comparison with the TSM analysis. In addition, one year of modelling results should cover most of the relevant scenarios of meteorological conditions. The model domain covers nearly all Europe (Figure 2), with a horizontal resolution of 0.25 x 0.125 degrees (lon x lat) and 14 vertical layers from the near surface to 7 km ASL. The high-resolution (0.1 x 0.1 degree) European emission inventory, Copernicus Atmosphere Monitoring Service-Regional Inventory-Version 4, developed by the Netherlands TNO (Kuenen et al., 2022), is deployed in the simulation. The gas phase chemistry is simulated using the Carbon Bond 6 Revision 2 mechanism (Hildebrandt Ruiz and Yarwood, 2013). The ISORROPIA model (Nenes et al., 1998) is used to simulate the thermodynamic and gas-particle partitioning of inorganic aerosols. Simulation of secondary organic aerosols is carried out using a 1.5-dimensional volatility basis set module (Koo et al., 2014). The CAMx model is driven by the hourly meteorology from the regional Weather

Research and Forecasting model (WRF, version 3.7), which is driven by and nudged to a 6-hourly reanalysis of global meteorology from the European Centre for Medium-range Weather Forecasts. The chemistry initial and boundary conditions for CAMx are provided by the MOZART4 global model (Horowitz et al., 2003). The CAMx model and the used configuration have been validated in many previous studies to well reproduce the air pollution over Europe (Daellenbach et al., 2023, 2020; Jiang et al., 2019b, 2019a). More details of model configuration and validation are given in our previous research (Daellenbach et al., 2020; Jiang et al., 2019b, 2019a).

3 Results and Discussion

The frequencies of the trajectories, without the concentrations, are presented in Figure 2. Figure 3 shows the yearly averaged results for the different species (BBOA, OOA, total organics, NH_4, NO_3, SO_4). For each species, the plot on the left-hand side displays the result of the TSM analysis, i.e., the specific source areas. On the right-hand side, respectively, we have plotted the specific local concentrations as simulated by CAMx (Jiang et al., 2019b). Additionally, emission inventories of a few selected species can be found in Figure S1. We have decided to focus here on the comparison with the simulated concentrations in order to obtain a comprehensive picture of both the source regions and those most affected by air pollution. Note that the scales for the TSM and CAMx results are different in Figure 3, in order to visualise better some of the patterns. Figure S2 shows the side-by-side comparisons with the same scaling. Figure 4 contains the seasonal plots for June, July, August (JJA) and December, January, February (DJF) of BBOA, NO_3, and SO_4, all of which we expected strong seasonality.

249 Firstly, looking at the frequency plot (Figure 2), we notice that the highest percentage of
250 trajectories are very close to the actual measurement stations, which is what we would expect. A
251 significant percentage of trajectories are over continental Europe, and there are also some over the
252 Atlantic. Overall, Figure 2 indicates a decent coverage of the air masses over the European domain
253 of interest.

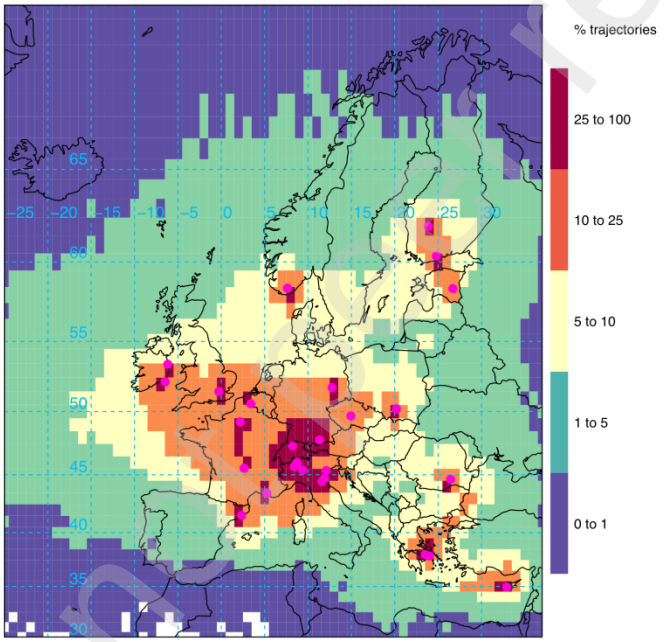

254

255 **Fig. 2.** Frequency plot of the trajectories without the concentrations. The colours indicate the
256 percentages of the total amount of trajectories passing through each grid cell. The pink dots
257 indicate the locations of the measurement sites.

258 It is important to note that in our analysis, all of the available ACSM/AMS data were used with
259 the CWT method in a single run, not accounting for different campaign durations and times. As
260 can be seen in Figure 1, some sites have much shorter campaigns and fewer data points in overall
261 comparison. Even though the CWT method weighs according to concentrations, not the number
262 of measurement points, this could still potentially lead to an underestimation of shorter campaigns.

263 To study this limitation, we have conducted different analyses, which are included in the
264 supplementary. Firstly, Figure S3 shows the year-round TSM analysis for only the stations in the
265 Po Valley, which had shorter campaigns compared to other regions. Figure S4 shows the results
266 of the TSM analysis for only the month of January with the most overlapping measurements in the
267 Po Valley, averaged over all years. Figure S5 again shows only the January average, excluding the
268 stations in Krakow and Bucharest. Comparing Figure S4 with the original DJF plots for BBOA,
269 NO_3, and SO_4, we see that the overall picture does not change significantly. Even excluding
270 Krakow and Bucharest from the analysis (Figure S5) only changes the scaling, not the source
271 regions highlighted. Comparing measurements from different times and of different durations
272 definitely poses a challenge, and we acknowledge this limitation, which is generally difficult to
273 quantify, in our analysis. But seeing that our results are sufficiently robust under different
274 circumstances gives us confidence in our approach and its ability to identify aerosol source regions,
275 while also allowing for a straightforward integration of datasets in the future. Nonetheless, we
276 highlight the need for long-term measurement datasets and a wide-spread network of stations.

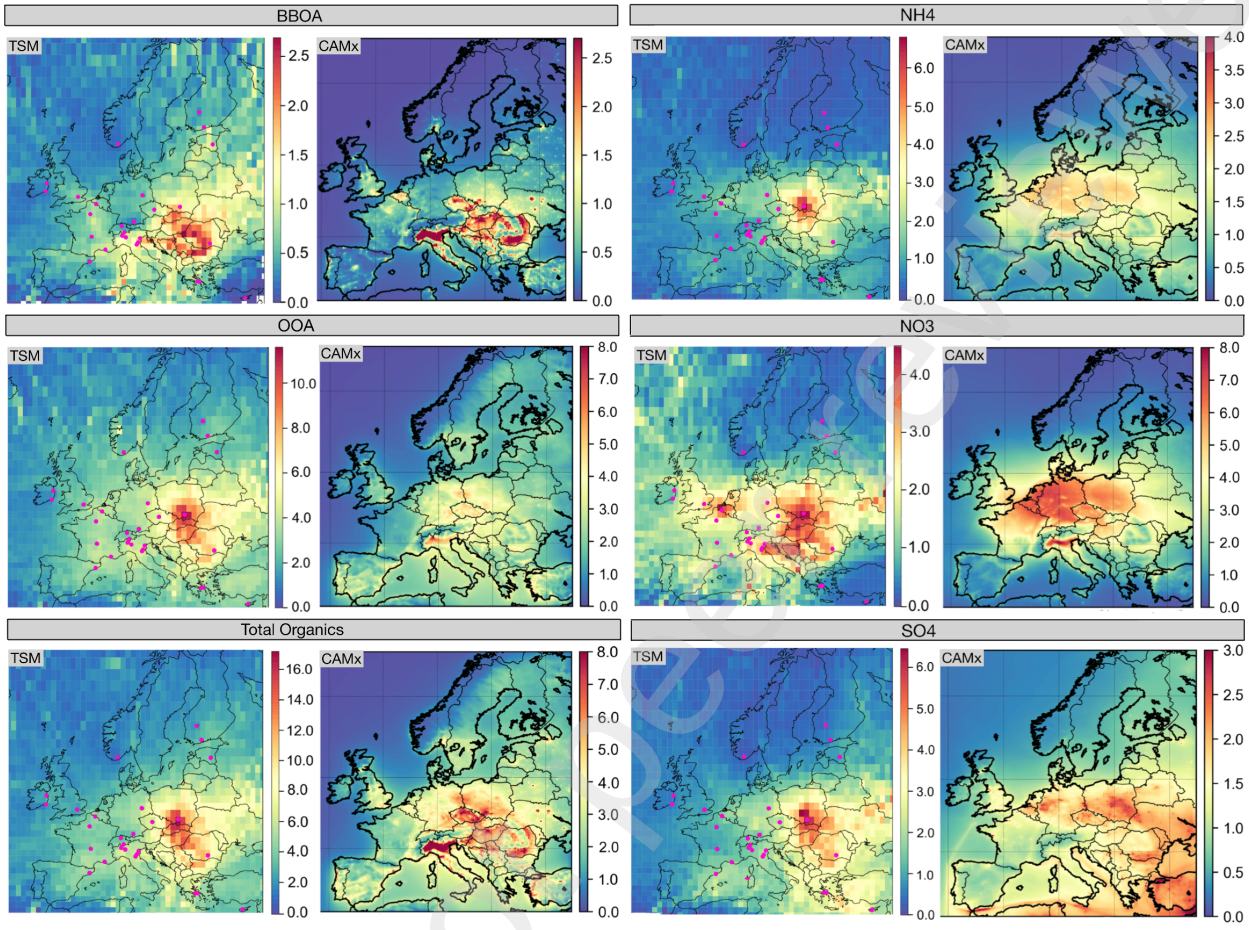

277

278 **Fig. 3.** Comparison of year-round TSM and CAMx results for BBOA, OOA, total OA, NH_4, NO_3,
279 and SO_4. Color scale is in $\mu g \cdot m^{-3}$.

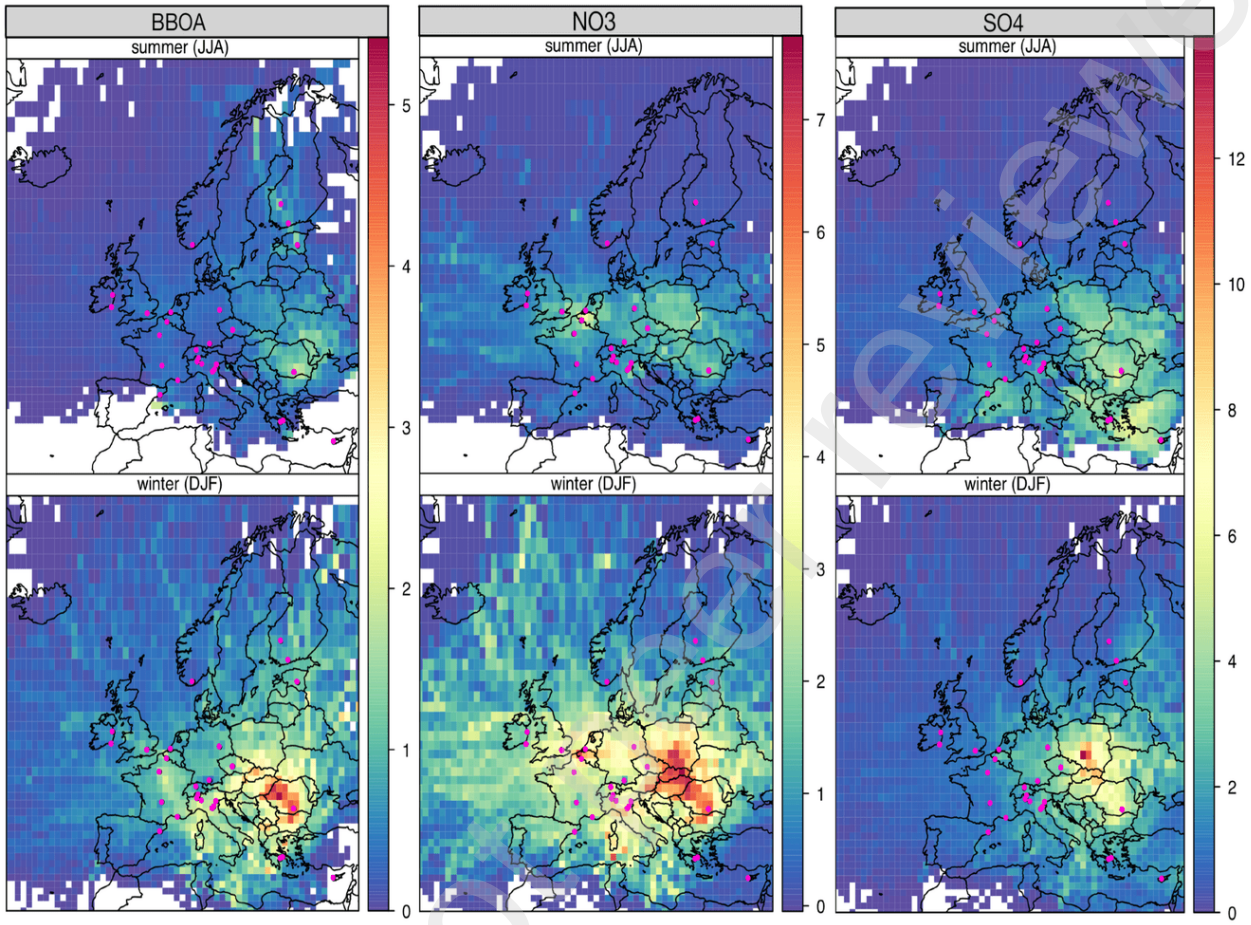

Fig. 4. Seasonal plots showing TSM results for BBOA, NO_3, and SO_4, with summer results on top and winter results on the bottom. Color scale is in $\mu g \cdot m^{-3}$.

3.1 BBOA

The results of the TSM analysis show that most of the contributions are from continental Europe. This is what we would expect since BBOA is only emitted over land. Most notably, the highest contributions come from eastern Europe, stretching from southern Poland to northern Greece. There is hardly anything from Western Europe.

In agreement with the TSM predictions, high BBOA concentrations were predicted in Eastern Europe by CAMx, in particular in Hungary, Romania, and the Balkans. This would suggest that

most of the BBOA emitted in those regions stays local as it's highly reactive in the atmosphere (Hennigan et al., 2010) and oxidises quickly. We can also observe concentration hotspots around major cities. The most significant difference between CAMx and TSM predictions can be observed in the Po Valley, where CAMx estimates a high BBOA concentration while not being elevated as a source region by the TSM analysis. When including the PMF results for Po Valley in the analysis we find a marginal increase in concentrations in those regions, compared to without (Figure S3). However, this region is still not at the same level of concentration as Eastern Europe. Potentially, the emission inventory for BBOA in the CAMx model is overestimated. Or, oxidation processes lead to the formation of OOA from BBOA, as described in Paglione et al. (2020). As we include multiple different sites, we could conclude that, relatively, the Po Valley is a less important source region of BBOA than Eastern Europe.

Figure 4 shows high BBOA concentrations in winter, indicating the importance of domestic heating sources. We can also see a high contribution from Finland in the summer.

3.2 OOA

Our analysis indicates that OOA mainly originates from continental Europe, with the highest concentrations observed in eastern Europe (from southern Poland to Romania). Although Chen et al. (2022) reported exceptionally high concentrations measured by the Krakow station, excluding this station from our analysis did not significantly alter the results, as illustrated in Figure S6. Therefore, we can confidently conclude that these regions indeed serve as hotspots for OOA.

CAMx also indicates high concentrations in eastern Europe, particularly in the Czech Republic, indicating a more local effect of OOA sources. This can also be seen in Hungary and southern

Romania, which are both elevated by the CAMx and TSM approaches. While the CAMx predicts high concentrations in the Po Valley, the TSM observed comparatively low contributions from this region. Once again, this could suggest that the Po Valley does not contribute much to the overall air pollution burden in Europe. Despite surrounding stations, the TSM did not predict significant contributions from Turkey, even though CAMx predicts high concentrations. This could possibly be due to limited trajectories passing through this region, as depicted in Figure 2.

3.3 Total organics

A distinct east-west contrast in OA concentrations is evident in both CAMx and TSM approaches, which indicates that OA is not transported over the entire continent. OA contributions primarily originate from continental Europe, notably southern Poland, extending to northern Bulgaria. The TSM highlights concentrations exceeding 16 $\mu g \cdot m^{-3}$ over Poland, compared to simulations reaching only up to 4 $\mu g \cdot m^{-3}$. This disparity can be attributed to exceptionally high concentrations around Krakow (Tobler et al., 2021), which might disproportionately affect the TSM analysis. However, performing the TSM analysis without the Krakow station (Figure S6) still highlights eastern Europe as the main source region. CAMx also predicts high OA concentrations in that region, in addition to the Benelux, parts of Germany, the Po Valley, and Turkey. This could either suggest a tendency for CAMx to underestimate actual OA levels in southern Poland, or indicate transport processes. Yet, multi-site observations from this region would be needed to confirm this tendency. CAMx also depicts localised high OA concentrations around major cities, beyond the resolution of the TSM analysis.

3.4 NH_4

Our TSM analysis shows the highest NH_4 contributions from the region in and around Krakow. Overall, eastern Europe is rather elevated, as are some regions in western Europe, such as the Benelux and Germany. The highest CAMx concentrations are over Belgium, Germany, Czechia, Po Valley, and Poland, with some slightly elevated concentrations over the southeast of the UK, northern France, Slovakia, Balkan regions, Ukraine, the south of Romania, and Turkey. Overall, both approaches show a consistent spatial distribution except for Po Valley, indicating that the emission inventory for CAMx is in agreement with the measurements except for Po Valley for the same reason as mentioned above. However, TSM model in general showed pronounced contributions of PM components in southern Poland, which leads to higher NH_4 concentrations than the CAMx model (Figure S2).

3.5 NO_3

In the TSM analysis, we observe significant contributions from northern France, the Benelux region, and eastern Europe, which align with the expected patterns given the influence of high NO_x and NH_3 emissions from urban areas, particularly those with heavy traffic. Surprisingly, we also detected relatively elevated contributions from the Atlantic, which prompted further investigation. Upon conducting our analysis without data from select stations in the UK, Ireland, Paris, and Lille, we found that this oceanic influence vanished, as illustrated in Figure S7. This suggests that these unexpected findings are likely artefacts of the TSM process. Additionally, trajectory analysis (see Figure 2) reveals a notable proportion of trajectories passing over the Atlantic, corroborating our

assessment. As expected, NO_3 exhibits a significant seasonal trend, with higher concentrations in winter due to enhanced partitioning at lower temperatures (Figure 4).

We observe that CAMx estimated concentrations of NO_3 are considerably higher than the TSM model across the UK, northern France, Germany, Czechia, and Po Valley with some agreements in the Benelux region, eastern Europe and southern Europe (Figure S2). The discrepancies of NO_3 from the CAMx model in the aforementioned regions are potentially caused by scarcities of measurements for TSM analysis and overestimations of the CAMx model.

3.6 SO_4

In winter, the TSM model predicts the highest concentrations over eastern Europe, particularly in Poland, likely due to industrial emissions and residential coal burning for heating (Figures 3 and 4). Significant contributions are also observed from the Mediterranean region, attributed to high ship emissions and enhanced photochemistry during the summer in this region (Figures 3 and 4). There is a match of hotspots between the TSM and CAMx simulations over Poland, the Balkans, the Mediterranean, and Turkey. However, the TSM model showed much higher concentrations than CAMx in eastern Europe due to the potential underestimation of the CAMx model from industrial and coal combustion sources. In addition, the CAMx model might slightly underestimate ship exhaust near the Aegean Sea and southwest of Turkey's coastline, resulting in relatively higher concentrations in these regions for the TSM model. Nevertheless, SO_4 could still be underestimated in the Balkans where coal power plants is a quite common source due to both the scarcity of measurements in this region and limitations of the emission inventories. The TSM

results for SO_4 in the UK show less pronounced contributions compared to the high concentrations predicted by CAMx, indicating a potential overestimation of SO_2 emissions in these regions.

4 Conclusion

In this study, we investigated various PM components, both organic (BBOA, OOA, and total OA) and inorganic (NH_4, NO_3, SO_4), and their long-range transport in Europe. Our aim was to identify their geographical origins by combining source apportionment results and measurements from 27 air quality observational sites with TSMs. Using numerous trajectories and receptors reduced uncertainties, providing a comprehensive analysis of source origins. We then compared these results to estimations of concentrations by the CAMx air quality model in Europe. However, we acknowledge the caveat of this analysis to combine several receptors with different time periods, and the fact that back trajectory analysis does not reproduce all atmospheric physicochemical processes.

Starting with the organic components, most contributions come from continental Europe. BBOA hotspots are around southern Poland to northern Greece. The main source regions as predicted by our analysis mostly align well with regions of high concentrations as simulated by CAMx, except for the Po Valley. Seasonally, concentrations are low in summer and high in winter, likely due to heating. For OOA, the highest contributions are also from eastern Europe, in particular southern Poland to Romania. The CAMx also highlights this region, but predicts overall lower absolute concentrations, which could indicate transport processes. Excluding the Poland station did not change results, suggesting this region is a major contributor, possibly also underestimated in the

CAMx model. The TSM analysis also shows discrepancies with the CAMx results in the Po Valley, potentially indicating an overestimation in the CAMx model, or transport processes. For total organics, the highest contributions are from southern Poland to Bulgaria, with a clear east-west contrast well captured by our TSM analysis. Overall, eastern Europe seems to be the most important contributor.

For inorganic components, NH4 shows high contributions from Poland, and the TSM results generally match predictions of regions with high concentrations from CAMx except for Po Valley. The NO_3 contribution is highest from northern France, Benelux, and eastern Europe due to NO_x emissions from traffic and agricultural emissions in Benelux. The CAMx results show higher concentrations than the TSM analysis in northern Europe, and Po Valley with good consistences in eastern Europe in general. TSM analysis showed lower NO_3 concentrations in summer, likely due to higher temperatures, photochemistry keeping NO_3 in the gas phase, and higher vertical dilution. SO_4 concentrations are high in Poland, likely from industrial and heating emissions, and over the Mediterranean, due to photochemistry and ship exhausts. This matches CAMx model highlights, though we do not find elevated concentrations over Benelux and Germany. Seasonally, SO_4 is higher in winter over Poland and in summer over the Mediterranean, supporting heating-related emissions and the photochemical transformation of SO_2 to SO_4, respectively.

In conclusion, we have developed a novel approach to take advantage of available large datasets to have a comprehensive picture of the geographical origins of different PM components, such as BBOA, OOA, total OA, NH_4, NO_3, and SO_4 across Europe. It demonstrated great consistency with the concentrations simulated by the CAMx model. With the help of more data available in the future, the results of this analysis could be used to validate and improve the emission inventories

of air quality chemical transport models. By understanding the intricate interplay between local emissions and long-range transport, stakeholders can implement informed strategies to improve air quality on a larger scale, protect human health, and safeguard ecosystems in both source and receptor regions.

Data availability

The code to execute the TSM analysis can be found in the supporting material. Raw data of the TSM data is publicly available through Zenodo: https://zenodo.org/records/6672710. The raw data of CAMx results are available through a request to the corresponding authors.

Acknowledgements

The authors gratefully acknowledge the Swiss data science center (grant C08-20, Aurora), the Swiss federal office of environment (FOEN) and the Joint Research Program of the Swiss National Science Foundation (SNSF grant no. 189883) for their financial support. We want to thank CNRS-INSU for supporting measurements performed at the SI-COPDD, and those within the long-term monitoring aerosol program SNO-CLAP, both of which are components of the ACTRIS French Research Infrastructure, and whose data is hosted at the AERIS data center (https://www.aeris-data.fr/). We further acknowledge EPA Ireland and the Department of Environment, Climate and Communications, Horizon Europe (grant no. 101081430 - PARIS), as well as the National Key Research and Development Program of China (2023YFC3710400), and the National Natural Science Foundation of China (42207122). Additionally, this work is supported by the Core

Program within the Romanian National Research Development and Innovation Plan 2022-2027, carried out with the support of MCID, project no. PN 23 05). Hasna Chebaicheb's PhD grant is supported by the LCSQA funded by the French Ministry of Environment. IMTNord Europe acknowledges financial support from the Labex CaPPA project, which is funded by the French National Research Agency (ANR) through the PIA (Programme d'Investissement d'Avenir) under contract ANR-11-LABX-0005-01, and the CLIMIBIO and ECRIN projects, both financed by the Regional Council "Hauts-de-France" and the European Regional Development Fund (ERDF). All co-authors participated in or supported by the COST COLOSSAL Action CA16109. The ATOLL site is one of the French ACTRIS National Facilities and contributes to the CARA program of the LCSQA funded by the French Ministry of Environment. Mikael Ehn, Liine Heikkinen, Minna Aurela, and Hilkka Timonen are funded by Research Council of Finland (grants 317380, 345982, 337549, 3570902 and 357905).

Lastly, we want to mention the invaluable work by the following people: Andres Alastuey (andres.alastuey@idaea.csic.es) from CSIC, Gregory Gille (gregory.gille@atmosud.org) from Atmosud, Erik Teinemaa (erik.teinemaa@klab.ee) from Estonian Environmental Research Centre (EERC), Anja Tremper (anja.tremper@imperial.ac.uk) and Max Priestman (m.priestman@imperial.ac.uk) from the MRC Centre for Environment and Health at Imperial College London.

References

Bressi, M., Cavalli, F., Putaud, J.P., Fröhlich, R., Petit, J.E., Aas, W., Äijälä, M., Alastuey, A., Allan, J.D., Aurela, M., Berico, M., Bougiatioti, A., Bukowiecki, N., Canonaco, F., Crenn, V., Dusanter, S., Ehn, M., Elsasser, M., Flentje, H., Graf, P., Green, D.C., Heikkinen, L., Hermann, H., Holzinger, R., Hueglin, C., Keernik, H., Kiendler-Scharr, A., Kubelová, L., Lunder, C., Maasikmets, M., Makeš, O., Malaguti, A., Mihalopoulos, N., Nicolas, J.B., O'Dowd, C., Ovadnevaite, J., Petralia, E., Poulain, L., Priestman, M., Riffault, V., Ripoll, A., Schlag, P., Schwarz, J., Sciare, J., Slowik, J., Sosedova, Y., Stavroulas, I., Teinemaa, E., Via, M., Vodička, P., Williams, P.I., Wiedensohler, A., Young, D.E., Zhang, S., Favez, O., Minguillón, M.C., Prevot, A.S.H., 2021. A European aerosol phenomenology - 7: High-time resolution chemical characteristics of submicron particulate matter across Europe. Atmos Environ X 10, 100108. https://doi.org/10.1016/J.AEAOA.2021.100108

Calvin, K., Dasgupta, D., Krinner, G., Mukherji, A., Thorne, P.W., Trisos, C., Romero, J., Aldunce, P., Barrett, K., Blanco, G., Cheung, W.W.L., Connors, S., Denton, F., Diongue-Niang, A., Dodman, D., Garschagen, M., Geden, O., Hayward, B., Jones, C., Jotzo, F., Krug, T., Lasco, R., Lee, Y.-Y., Masson-Delmotte, V., Meinshausen, M., Mintenbeck, K., Mokssit, A., Otto, F.E.L., Pathak, M., Pirani, A., Poloczanska, E., Pörtner, H.-O., Revi, A., Roberts, D.C., Roy, J., Ruane, A.C., Skea, J., Shukla, P.R., Slade, R., Slangen, A., Sokona, Y., Sörensson, A.A., Tignor, M., van Vuuren, D., Wei, Y.-M., Winkler, H., Zhai, P., Zommers, Z., Hourcade, J.-C., Johnson, F.X., Pachauri, S., Simpson, N.P., Singh, C., Thomas, A., Totin, E., Alegría, A., Armour, K., Bednar-Friedl, B., Blok, K., Cissé, G., Dentener, F., Eriksen, S., Fischer, E.,

Garner, G., Guivarch, C., Haasnoot, M., Hansen, G., Hauser, M., Hawkins, E., Hermans, T., Kopp, R., Leprince-Ringuet, N., Lewis, J., Ley, D., Ludden, C., Niamir, L., Nicholls, Z., Some, S., Szopa, S., Trewin, B., van der Wijst, K.-I., Winter, G., Witting, M., Birt, A., Ha, M., 2023. IPCC, 2023: Climate Change 2023: Synthesis Report. Contribution of Working Groups I, II and III to the Sixth Assessment Report of the Intergovernmental Panel on Climate Change [Core Writing Team, H. Lee and J. Romero (eds.)]. IPCC, Geneva, Switzerland. https://doi.org/10.59327/IPCC/AR6-9789291691647

Carslaw, D., 2019. The openair manual open-source tools for analysing air pollutiondata.

Chen, G., Canonaco, F., Tobler, A., Aas, W., Alastuey, A., Allan, J., Atabakhsh, S., Aurela, M., Baltensperger, U., Bougiatioti, A., De Brito, J.F., Ceburnis, D., Chazeau, B., Chebaicheb, H., Daellenbach, K.R., Ehn, M., El Haddad, I., Eleftheriadis, K., Favez, O., Flentje, H., Font, A., Fossum, K., Freney, E., Gini, M., Green, D.C., Heikkinen, L., Herrmann, H., Kalogridis, A.-C., Keernik, H., Lhotka, R., Lin, C., Lunder, C., Maasikmets, M., Manousakas, M.I., Marchand, N., Marin, C., Marmureanu, L., Mihalopoulos, N., Močnik, G., Nęcki, J., O'Dowd, C., Ovadnevaite, J., Peter, T., Petit, J.-E., Pikridas, M., Matthew Platt, S., Pokorná, P., Poulain, L., Priestman, M., Riffault, V., Rinaldi, M., Różański, K., Schwarz, J., Sciare, J., Simon, L., Skiba, A., Slowik, J.G., Sosedova, Y., Stavroulas, I., Styszko, K., Teinemaa, E., Timonen, H., Tremper, A., Vasilescu, J., Via, M., Vodička, P., Wiedensohler, A., Zografou, O., Cruz Minguillón, M., Prévôt, A.S.H., 2022. European aerosol phenomenology − 8: Harmonised source apportionment of organic aerosol using 22 Year-long ACSM/AMS datasets. Environ Int 166, 107325. https://doi.org/10.1016/j.envint.2022.107325

493 Chen, Y., Beig, G., Archer-Nicholls, S., Drysdale, W., Acton, W.J.F., Lowe, D., Nelson, B., Lee,
494 J., Ran, L., Wang, Y., Wu, Z., Sahu, S.K., Sokhi, R.S., Singh, V., Gadi, R., Nicholas Hewitt,
495 C., Nemitz, E., Archibald, A., McFiggans, G., Wild, O., 2021. Avoiding high ozone pollution
496 in Delhi, India. Faraday Discuss 226, 502–514. https://doi.org/10.1039/D0FD00079E
497 Crippa, M., Canonaco, F., Lanz, V.A., Äijälä, M., Allan, J.D., Carbone, S., Capes, G., Ceburnis,
498 D., Dall'Osto, M., Day, D.A., DeCarlo, P.F., Ehn, M., Eriksson, A., Freney, E.,
499 Hildebrandt Ruiz, L., Hillamo, R., Jimenez, J.L., Junninen, H., Kiendler-Scharr, A.,
500 Kortelainen, A.-M., Kulmala, M., Laaksonen, A., Mensah, A.A., Mohr, C., Nemitz, E.,
501 O'Dowd, C., Ovadnevaite, J., Pandis, S.N., Petäjä, T., Poulain, L., Saarikoski, S.,
502 Sellegri, K., Swietlicki, E., Tiitta, P., Worsnop, D.R., Baltensperger, U., Prévôt, A.S.H.H.,
503 2014. Organic aerosol components derived from 25 AMS data sets across Europe using a
504 consistent ME-2 based source apportionment approach. Atmos Chem Phys 14, 6159–6176.
505 https://doi.org/10.5194/acp-14-6159-2014
506 Daellenbach, K.R., Manousakas, M., Jiang, J., Cui, T., Chen, Y., El Haddad, I., Fermo, P., Colombi,
507 C., Prévôt, A.S.H., 2023. Organic aerosol sources in the Milan metropolitan area – Receptor
508 modelling based on field observations and air quality modelling. Atmos Environ 307, 119799.
509 https://doi.org/10.1016/j.atmosenv.2023.119799
510 Daellenbach, K.R., Uzu, G., Jiang, J., Cassagnes, L.-E., Leni, Z., Vlachou, A., Stefenelli, G.,
511 Canonaco, F., Weber, S., Segers, A., Kuenen, J.J.P., Schaap, M., Favez, O., Albinet, A.,
512 Aksoyoglu, S., Dommen, J., Baltensperger, U., Geiser, M., El Haddad, I., Jaffrezo, J.-L.,
513 Prévôt, A.S.H., 2020. Sources of particulate-matter air pollution and its oxidative potential in
514 Europe. Nature 587, 414–419. https://doi.org/10.1038/s41586-020-2902-8

515 Drewnick, F., Hings, S.S., DeCarlo, P., Jayne, J.T., Gonin, M., Fuhrer, K., Weimer, S., Jimenez,
516 J.L., Demerjian, K.L., Borrmann, S., Worsnop, D.R., 2005. A New Time-of-Flight Aerosol
517 Mass Spectrometer (TOF-AMS)—Instrument Description and First Field Deployment.
518 Aerosol Science and Technology 39, 637–658. https://doi.org/10.1080/02786820500182040
519 Escudero, M., Stein, A.F., Draxler, R.R., Querol, X., Alastuey, A., Castillo, S., Avila, A., 2011.
520 Source apportionment for African dust outbreaks over the Western Mediterranean using the
521 HYSPLIT model. Atmos Res 99, 518–527. https://doi.org/10.1016/j.atmosres.2010.12.002
522 Fröhlich, R., Cubison, M.J., Slowik, J.G., Bukowiecki, N., Prévôt, A.S.H., Baltensperger, U.,
523 Schneider, J., Kimmel, J.R., Gonin, M., Rohner, U., Worsnop, D.R., Jayne, J.T., 2013. The
524 ToF-ACSM: a portable aerosol chemical speciation monitor with TOFMS detection. Atmos
525 Meas Tech 6, 3225–3241. https://doi.org/10.5194/amt-6-3225-2013
526 GDAS, n.d. Global Data Assimilation System (GDAS) | National Centers for Environmental
527 Information (NCEI) [WWW Document]. URL https://www.ncei.noaa.gov/products/weather-
528 climate-models/global-data-assimilation (accessed 1.11.25).
529 Harrison, R.M., Yin, J., 2000. Particulate matter in the atmosphere: which particle properties are
530 important for its effects on health? Science of The Total Environment 249, 85–101.
531 https://doi.org/10.1016/S0048-9697(99)00513-6
532 Hennigan, C.J., Sullivan, A.P., Collett, J.L., Robinson, A.L., 2010. Levoglucosan stability in
533 biomass burning particles exposed to hydroxyl radicals. Geophys Res Lett 37, 2–5.
534 https://doi.org/10.1029/2010GL043088
535 Hildebrandt Ruiz, L., Yarwood, G., 2013. Interactions between organic aerosol and NOy:
536 Influence on oxidant production. Final report prepared for the Texas Air Quality Research

Program (Project 12-012) by the University of Texas at Austin and ENVIRON International Corporation.

Horowitz, L.W., Walters, S., Mauzerall, D.L., Emmons, L.K., Rasch, P.J., Granier, C., Tie, X., Lamarque, J., Schultz, M.G., Tyndall, G.S., Orlando, J.J., Brasseur, G.P., 2003. A global simulation of tropospheric ozone and related tracers: Description and evaluation of MOZART, version 2. Journal of Geophysical Research: Atmospheres 108. https://doi.org/10.1029/2002JD002853

Hsu, Y.-K., Holsen, T.M., Hopke, P.K., 2003. Comparison of hybrid receptor models to locate PCB sources in Chicago. Atmos Environ 37, 545–562. https://doi.org/10.1016/S1352-2310(02)00886-5

Jiang, J., Aksoyoglu, S., Ciarelli, G., Oikonomakis, E., El-Haddad, I., Canonaco, F., O'Dowd, C., Ovadnevaite, J., Minguillón, M.C., Baltensperger, U., Prévôt, A.S.H., 2019a. Effects of two different biogenic emission models on modelled ozone and aerosol concentrations in Europe. Atmos Chem Phys 19, 3747–3768. https://doi.org/10.5194/acp-19-3747-2019

Jiang, J., Aksoyoglu, S., El-Haddad, I., Ciarelli, G., Denier van der Gon, H.A.C., Canonaco, F., Gilardoni, S., Paglione, M., Minguillón, M.C., Favez, O., Zhang, Y., Marchand, N., Hao, L., Virtanen, A., Florou, K., O'Dowd, C., Ovadnevaite, J., Baltensperger, U., Prévôt, A.S.H., 2019b. Sources of organic aerosols in Europe: a modeling study using CAMx with modified volatility basis set scheme. Atmos Chem Phys 19, 15247–15270. https://doi.org/10.5194/acp-19-15247-2019

Jimenez, J.L., Canagaratna, M.R., Donahue, N.M., Prevot, A.S.H.H., Zhang, Q., Kroll, J.H., DeCarlo, P.F., Allan, J.D., Coe, H., Ng, N.L., Aiken, A.C., Docherty, K.S., Ulbrich, I.M.,

559 Grieshop, A.P., Robinson, A.L., Duplissy, J., Smith, J.D., Wilson, K.R., Lanz, V.A., Hueglin,
560 C., Sun, Y.L., Tian, J., Laaksonen, A., Raatikainen, T., Rautiainen, J., Vaattovaara, P., Ehn,
561 M., Kulmala, M., Tomlinson, J.M., Collins, D.R., Cubison, M.J., Dunlea, J., Huffman, J.A.,
562 Onasch, T.B., Alfarra, M.R., Williams, P.I., Bower, K., Kondo, Y., Schneider, J., Drewnick,
563 F., Borrmann, S., Weimer, S., Demerjian, K., Salcedo, D., Cottrell, L., Griffin, R., Takami,
564 A., Miyoshi, T., Hatakeyama, S., Shimono, A., Sun, J.Y., Zhang, Y.M., Dzepina, K., Kimmel,
565 J.R., Sueper, D., Jayne, J.T., Herndon, S.C., Trimborn, A.M., Williams, L.R., Wood, E.C.,
566 Middlebrook, A.M., Kolb, C.E., Baltensperger, U., Worsnop, D.R., Dunlea, E.J., Huffman,
567 J.A., Onasch, T.B., Alfarra, M.R., Williams, P.I., Bower, K., Kondo, Y., Schneider, J.,
568 Drewnick, F., Borrmann, S., Weimer, S., Demerjian, K., Salcedo, D., Cottrell, L., Griffin, R.,
569 Takami, A., Miyoshi, T., Hatakeyama, S., Shimono, A., Sun, J.Y., Zhang, Y.M., Dzepina, K.,
570 Kimmel, J.R., Sueper, D., Jayne, J.T., Herndon, S.C., Trimborn, A.M., Williams, L.R., Wood,
571 E.C., Middlebrook, A.M., Kolb, C.E., Baltensperger, U., Worsnop, D.R., 2009. Evolution of
572 Organic Aerosols in the Atmosphere. Science (1979) 326, 1525–1529.
573 https://doi.org/10.1126/science.1180353

574 Koo, B., Knipping, E., Yarwood, G., 2014. 1.5-Dimensional volatility basis set approach for
575 modeling organic aerosol in CAMx and CMAQ. Atmos Environ 95, 158–164.
576 https://doi.org/10.1016/j.atmosenv.2014.06.031

577 Kuenen, J., Dellaert, S., Visschedijk, A., Jalkanen, J.-P., Super, I., Denier van der Gon, H., 2022.
578 CAMS-REG-v4: a state-of-the-art high-resolution European emission inventory for air
579 quality modelling. Earth Syst Sci Data 14, 491–515. https://doi.org/10.5194/essd-14-491-
580 2022

581 Lee, S., Ashbaugh, L., 2007. Comparison of multi-receptor and single-receptor trajectory source
582 apportionment (TSA) methods using artificial sources. Atmos Environ 41, 1119–1127.
583 https://doi.org/10.1016/j.atmosenv.2006.10.019
584 Liu, X., Lara, R., Dufresne, M., Wu, L., Zhang, X., Wang, T., Monge, M., Reche, C., Di Leo, A.,
585 Lanzani, G., Colombi, C., Font, A., Sheehan, A., Green, D.C., Makkonen, U., Sauvage, S.,
586 Salameh, T., Petit, J.-E., Chatain, M., Coe, H., Hou, S., Harrison, R., Hopke, P.K., Petäjä, T.,
587 Alastuey, A., Querol, X., 2024. Variability of ambient air ammonia in urban Europe (Finland,
588 France, Italy, Spain, and the UK). Environ Int 185, 108519.
589 https://doi.org/10.1016/j.envint.2024.108519
590 Lupu, A., Maenhaut, W., 2002. Application and comparison of two statistical trajectory techniques
591 for identification of source regions of atmospheric aerosol species. Atmos Environ 36, 5607–
592 5618. https://doi.org/10.1016/S1352-2310(02)00697-0
593 Mitsakou, C., Housiadas, C., Eleftheriadis, K., Vratolis, S., Helmis, C., Asimakopoulos, D., 2007.
594 Lung deposition of fine and ultrafine particles outdoors and indoors during a cooking event
595 and a no activity period. Indoor Air 17, 143–152. https://doi.org/10.1111/j.1600-
596 0668.2006.00464.x
597 Nenes, A., Pandis, S.N., Pilinis, C., 1998. ISORROPIA: A New Thermodynamic Equilibrium
598 Model for Multiphase Multicomponent Inorganic Aerosols. Aquat Geochem 4, 123–152.
599 https://doi.org/10.1023/A:1009604003981
600 Ng, N.L., Herndon, S.C., Trimborn, A., Canagaratna, M.R., Croteau, P.L., Onasch, T.B., Sueper,
601 D., Worsnop, D.R., Zhang, Q., Sun, Y.L., Jayne, J.T., 2011. An Aerosol Chemical Speciation
602 Monitor (ACSM) for Routine Monitoring of the Composition and Mass Concentrations of

603 Ambient Aerosol. Aerosol Science and Technology 45, 780–794.
604 https://doi.org/10.1080/02786826.2011.560211
605 NOAA, n.d. HYSPLIT – Air Resources Laboratory [WWW Document]. URL
606 https://www.arl.noaa.gov/hysplit/ (accessed 1.11.25).
607 Paglione, M., Gilardoni, S., Rinaldi, M., Decesari, S., Zanca, N., Sandrini, S., Giulianelli, L.,
608 Bacco, D., Ferrari, S., Poluzzi, V., Scotto, F., Trentini, A., Poulain, L., Herrmann, H.,
609 Wiedensohler, A., Canonaco, F., Prévôt, A.S.H., Massoli, P., Carbone, C., Facchini, M.C.,
610 Fuzzi, S., 2020. The impact of biomass burning and aqueous-phase processing on air quality:
611 a multi-year source apportionment study in the Po Valley, Italy. Atmos Chem Phys 20, 1233–
612 1254. https://doi.org/10.5194/acp-20-1233-2020
613 Salvador, P., Artíñano, B., Pio, C., Afonso, J., Legrand, M., Puxbaum, H., Hammer, S., 2010.
614 Evaluation of aerosol sources at European high altitude background sites with trajectory
615 statistical methods. Atmos Environ 44, 2316–2329.
616 https://doi.org/10.1016/j.atmosenv.2010.03.042
617 Salvador, P., Artíñano, B., Querol, X., Alastuey, A., 2008. A combined analysis of backward
618 trajectories and aerosol chemistry to characterise long-range transport episodes of particulate
619 matter: The Madrid air basin, a case study. Science of The Total Environment 390, 495–506.
620 https://doi.org/10.1016/j.scitotenv.2007.10.052
621 Samoli, E., Atkinson, R.W., Analitis, A., Fuller, G.W., Green, D.C., Mudway, I., Anderson, H.R.,
622 Kelly, F.J., 2016. Associations of short-term exposure to traffic-related air pollution with
623 cardiovascular and respiratory hospital admissions in London, UK. Occup Environ Med 73,
624 300–307. https://doi.org/10.1136/oemed-2015-103136

625 Stein, A.F., Draxler, R.R., Rolph, G.D., Stunder, B.J.B., Cohen, M.D., Ngan, F., 2015. NOAA's
626 HYSPLIT Atmospheric Transport and Dispersion Modeling System. Bull Am Meteorol Soc
627 96, 2059–2077. https://doi.org/10.1175/BAMS-D-14-00110.1
628 Stohl, A., 1996. Trajectory statistics-A new method to establish source-receptor relationships of
629 air pollutants and its application to the transport of particulate sulfate in Europe. Atmos
630 Environ 30, 579–587. https://doi.org/10.1016/1352-2310(95)00314-2
631 Tobler, A.K., Skiba, A., Canonaco, F., Močnik, G., Rai, P., Chen, G., Bartyzel, J., Zimnoch, M.,
632 Styszko, K., Nęcki, J., Furger, M., Rózański, K., Baltensperger, U., Slowik, J.G., Prevot,
633 A.S.H., 2021. Characterization of non-refractory (NR) PM<inf>1</inf>and source
634 apportionment of organic aerosol in Kraków, Poland. Atmos Chem Phys 21.
635 https://doi.org/10.5194/acp-21-14893-2021
636 Wilks, D.S., 2019. Statistical Methods in the Atmospheric Sciences, Fourth Edition, Statistical
637 Methods in the Atmospheric Sciences, Fourth Edition. Elsevier.
638 https://doi.org/10.1016/C2017-0-03921-6
639 Yarwood, G., Wilson, G., Emery, C., Morris, R., 2024. User's Guide COMPREHENSIVE AIR
640 QUALITY MODEL WITH EXTENSIONS. Ramboll Environment and Health.
641